

## Bounds on effective conductivities of heterogeneous media with graded constituents

J. Wang,\* H. L. Duan, and X. Yi

*LTCS and Department of Mechanics and Engineering Science, Peking University, Beijing 100871, People's Republic of China*

(Received 10 September 2005; revised manuscript received 29 December 2005; published 30 March 2006)

The bounds on the effective conductivities of heterogeneous media containing discretely suspended particles with a graded interphase or graded particles are presented through introducing comparison materials. The microstructures of the comparison materials are different from those of the considered heterogeneous media. The comparison materials provide a means of obtaining optimized narrow bounds. The effective conductivities of these composites are also predicted using the composite sphere assemblage (CSA) model. It is shown that the CSA predictions are within the appropriate bounds for the considered media.

DOI: [10.1103/PhysRevB.73.104208](https://doi.org/10.1103/PhysRevB.73.104208)

PACS number(s): 77.84.Lf, 41.20.Cv, 77.22.-d

### I. INTRODUCTION

Predicting the effective physical properties (e.g., the dielectric constant, the thermal or electric conductivity, and the effective elastic constants, etc.) of heterogeneous media has been a subject of scientific and engineering interest spanning more than a century, attracting the attention of many luminaries such as Maxwell, Rayleigh, and Einstein.<sup>1-3</sup> Many approaches and predictive schemes have been proposed and summarized in articles and textbooks.<sup>4-15</sup> Among these approaches, bounding the possible range of the effective properties is of fundamental importance. Appropriate bounds can be used to assess a particular predictive scheme, and they can also constitute an accurate prediction of the effective properties when the bounding range is sufficiently narrow. Hashin and Shtrikman<sup>6</sup> gave the lower and upper bounds on the effective conductivity of a multiphase heterogeneous medium (each phase of the heterogeneous medium is homogeneous) by introducing a homogeneous comparison material. The Hashin-Shtrikman bounds only rely on the properties and volume fractions of the constituents of a heterogeneous medium but not on the microstructure. With increased microstructural information, the bounds can be narrowed, increasing further the precision of the prediction they provide.<sup>7,9,12-15</sup> Moreover, bounds for nonlinear heterogeneous media have been developed. For example, Ponte Castañeda<sup>12</sup> obtained the three-point bounds and other estimates for strongly nonlinear heterogeneous media by the variational procedure making use of the effective properties of the linear comparison materials.

The effective conductivities of graded heterogeneous media have been paid a lot of attention<sup>16-23</sup> due to the increasing interest in functionally graded materials (FGMs) which have various engineering applications.<sup>24</sup> The main characteristic that distinguishes FGMs from conventional composite materials is the tailoring of the graded composition and microstructure to achieve the desired function.<sup>25</sup> For mechanical properties, the main advantages of a graded material profile range from the improved bonding strength and toughness to wear and corrosion resistance.<sup>23,26</sup> In nature, there also exist many graded materials, such as biological cells because of the inhomogeneous compartments inside the nuclei.<sup>27</sup> In addition, in most granular composites, the interface between the particles and the matrix may not be very sharp and smooth due to the diffusion and surface roughness.<sup>23,26,28</sup>

The change in the composition and/or microstructure induces the gradients of the properties of the materials.<sup>28</sup>

Recently, core-shell nanoparticles with uniform or non-uniform compositions have attracted the attention of researchers in various fields.<sup>29-31</sup> The alloyed semiconductor quantum dots<sup>30,32</sup> with graded internal structures have been prepared to achieve continuous tuning of the optical properties without changing the particle size. For this kind of alloyed nanostructure, three factors, namely, the particle size, the composition, and the internal structure, can be used to control the quantum confinement effect and to provide novel properties not available from the individual components.<sup>30,32</sup> Goncharenko<sup>33</sup> calculated the effective dielectric responses of composites containing core-shell particles analytically and numerically based on the Clausius-Mossotti/Maxwell Garnett theory. By using *ab initio* calculations for Ge and Si nanocrystals embedded in a SiC matrix, Weissker *et al.*<sup>34</sup> demonstrated that the effective-medium theory works well for crystallites with the minimum size about 1 nm. Core-shell particles can be used as a constituent part of a composite medium, besides being functional devices on their own.<sup>29,31,33,35-37</sup> Therefore the effect of the graded properties of core-shell nanoparticles on the effective conductivities (e.g., the dielectric response) of the heterogeneous media in which they are embedded is important in the application of these particles.

The Hashin-Shtrikman bounds<sup>6</sup> are for a heterogeneous medium in which each constituent phase has a definite conductivity and a definite volume fraction. Therefore, generally, they cannot be applied to heterogeneous media with graded constituents. It is noted that Quintanilla and Torquato<sup>16</sup> presented certain  $n$ -point correlation functions for graded composites containing inhomogeneous distribution of spheres whose density obeys any specified variation in volume fraction. These functions are essential in the study of the effective properties of the statistically inhomogeneous random media. Wei *et al.*<sup>18</sup> and Dong *et al.*<sup>19</sup> predicted the effective dielectric constants of heterogeneous media containing spherical or cylindrical particles with different dielectric profiles (e.g., simple power-law, linear, and exponential profiles) by using Landau's formula<sup>5</sup> and the differential effective dipole approximation. Lutz and Zimmerman<sup>23</sup> studied the effect of a graded interphase zone on the conductivity of a particulate composite. Recently, Wu *et al.*<sup>38</sup> predicted the upper and lower bounds on the effective elastic properties for

a composite containing particles with a graded interphase by introducing a *comparison material* with a microstructure different from that of the composite. In this paper, also by introducing comparison materials with microstructures different from those of the considered heterogeneous media, we present the bounds on the effective conductivities of heterogeneous media comprising continuous matrices and discretely suspended graded particles or homogeneous particles with graded interphases. Moreover, the composite sphere assemblage (CSA) model is also used to estimate the effective conductivities of these heterogeneous media and the predictions from the CSA are compared with the bounds.

This paper is organized as follows. In the next section, the theoretical framework leading to the upper and lower bounds is presented. The numerical results of the bounds and the CSA predictions for some graded interphases and graded particles are shown in Secs. III and IV, respectively. Finally, some conclusions are drawn in Sec. V.

## II. THEORY OF UPPER AND LOWER BOUNDS FOR GRADED MEDIA

### A. Upper and lower bounds

As pointed out by Hashin and Shtrikman,<sup>6</sup> the problems for predicting the effective magnetic permeability, dielectric constant, electric conductivity, heat conductivity, and diffusivity of heterogeneous media are mathematically analogous. Thus we consider an electric conduction problem of a heterogeneous media. Let  $\mathbf{J}(\mathbf{x})$  denote the local flux at position  $\mathbf{x}$ , and  $\mathbf{E}(\mathbf{x})$  denote the local field intensity. Under the steady-state condition with no source, the conservation of energy requires that  $\mathbf{J}(\mathbf{x})$  be divergence-free, i.e.,  $\nabla \cdot \mathbf{J}(\mathbf{x}) = 0$ . The intensity field  $\mathbf{E}(\mathbf{x})$  is taken to be irrotational, i.e.,  $\nabla \times \mathbf{E}(\mathbf{x}) = \mathbf{0}$ , where  $\mathbf{E}(\mathbf{x}) = -\nabla\Phi(\mathbf{x})$ , and  $\Phi(\mathbf{x})$  is the potential field. The linear constitutive relation, which relates  $\mathbf{J}(\mathbf{x})$  to  $\mathbf{E}(\mathbf{x})$ , is  $\mathbf{J}(\mathbf{x}) = \boldsymbol{\sigma}(\mathbf{x}) \cdot \mathbf{E}(\mathbf{x})$  or  $\mathbf{E}(\mathbf{x}) = \boldsymbol{\rho}(\mathbf{x}) \cdot \mathbf{J}(\mathbf{x})$ , where  $\boldsymbol{\sigma}(\mathbf{x})$  and  $\boldsymbol{\rho}(\mathbf{x})$  are the second-order conductivity and resistivity tensors, respectively, and they are reciprocal. The energy dissipated per unit volume in a material is a non-negative quantity that is proportional to the inner product of the intensity field and flux field,<sup>15</sup> i.e.,

$$w(\mathbf{x}) = \frac{1}{2} \mathbf{E}(\mathbf{x}) \cdot \mathbf{J}(\mathbf{x}) = \frac{1}{2} \mathbf{E}(\mathbf{x}) \cdot \boldsymbol{\sigma}(\mathbf{x}) \cdot \mathbf{E}(\mathbf{x}) \geq 0$$

or

$$w(\mathbf{x}) = \frac{1}{2} \mathbf{E}(\mathbf{x}) \cdot \mathbf{J}(\mathbf{x}) = \frac{1}{2} \mathbf{J}(\mathbf{x}) \cdot \boldsymbol{\rho}(\mathbf{x}) \cdot \mathbf{J}(\mathbf{x}) \geq 0$$

The above basic equations together with the corresponding boundary and interface conditions can be used to solve the local fields for the steady-state conduction problem.

We consider a representative volume element (RVE) with the exterior boundary  $S$  [Fig. 1(a)] of an *ergodic* heterogeneous medium,<sup>15</sup> hereinafter referred to as the real material, consisting of a continuous matrix and discretely suspended homogeneous particles with a graded interphase or graded particles without an interphase. The local conductivity and resistivity tensors of the heterogeneous medium at a point  $\mathbf{x}$  are denoted by  $\boldsymbol{\sigma}(\mathbf{x})$  and  $\boldsymbol{\rho}(\mathbf{x})$ , respectively. Now introduce an inhomogeneous, but also *ergodic*, comparison material

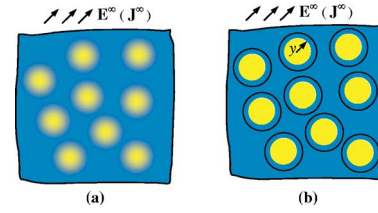


FIG. 1. (Color online) A heterogeneous medium with a continuous matrix and discretely suspended homogeneous particles with a graded interphase or graded particles (a), and the comparison material with a continuous matrix and discretely suspended homogeneous (nongraded) particles (b). For the meaning of  $\mathbf{x}$  in Fig. 1(b) see the text.

with a microstructure different from that of the considered heterogeneous medium. For example, the comparison material consists of a continuous and homogeneous matrix and discretely suspended homogeneous (nongraded) particles [Fig. 1(b)]. The conductivity and resistivity tensors at a point  $\mathbf{x}$  in the comparison material are denoted by  $\boldsymbol{\sigma}^0(\mathbf{x})$  and  $\boldsymbol{\rho}_0(\mathbf{x})$ , respectively [Fig. 1(b)].

Apply the boundary condition  $\Phi|_S = -\mathbf{E}^\infty \cdot \mathbf{x}$  on the exterior boundary of the RVEs of the real and the comparison materials in Figs. 1(a) and 1(b), where the subscript  $S$  denotes the external boundary of the RVEs, and  $\mathbf{E}^\infty$  is the uniform externally applied intensity vector. Under this prescribed boundary condition, the local intensity and local flux vectors in the real heterogeneous material are denoted by  $\mathbf{E}(\mathbf{x})$  and  $\mathbf{J}(\mathbf{x})$ , respectively; and those in the comparison material are denoted by  $\mathbf{E}^0(\mathbf{x})$  and  $\mathbf{J}_0(\mathbf{x})$ , respectively. Then it follows that

$$\langle \mathbf{E}(\mathbf{x}) \rangle = \langle \mathbf{E}^0(\mathbf{x}) \rangle = \mathbf{E}^\infty, \quad (1)$$

where  $\langle \cdot \rangle$  denotes the volume average of the corresponding quantity. According to Eq. (1), the macroscopic energy  $\tilde{W}_R$  of the real material is<sup>15</sup>

$$\tilde{W}_R = \frac{1}{2} \langle \mathbf{E}(\mathbf{x}) \rangle \cdot \bar{\boldsymbol{\sigma}} \cdot \langle \mathbf{E}(\mathbf{x}) \rangle = \frac{1}{2} \mathbf{E}^\infty \cdot \bar{\boldsymbol{\sigma}} \cdot \mathbf{E}^\infty, \quad (2)$$

where  $\bar{\boldsymbol{\sigma}}$  is the effective conductivity tensor of the real material. Similarly, the macroscopic energy  $\tilde{W}_C$  of the comparison material is<sup>15</sup>

$$\tilde{W}_C = \frac{1}{2} \langle \mathbf{E}^0(\mathbf{x}) \rangle \cdot \bar{\boldsymbol{\sigma}}^0 \cdot \langle \mathbf{E}^0(\mathbf{x}) \rangle = \frac{1}{2} \mathbf{E}^\infty \cdot \bar{\boldsymbol{\sigma}}^0 \cdot \mathbf{E}^\infty, \quad (3)$$

where  $\bar{\boldsymbol{\sigma}}^0$  is the effective conductivity tensor of the comparison material. Using Eq. (14.31) in the book of Torquato<sup>15</sup> and Eqs. (2) and (3), the energy difference  $\tilde{W}_R - \tilde{W}_C$  can be expressed as

$$\begin{aligned} & \mathbf{E}^\infty \cdot (\bar{\boldsymbol{\sigma}} - \bar{\boldsymbol{\sigma}}^0) \cdot \mathbf{E}^\infty \\ &= \langle \mathbf{E} \cdot \Delta \boldsymbol{\sigma} \cdot \mathbf{E} \rangle + \langle \Delta \mathbf{E} \cdot \boldsymbol{\sigma}^0 \cdot \Delta \mathbf{E} \rangle \\ & \quad + \langle \mathbf{E}^0 \cdot \boldsymbol{\sigma}^0 \cdot \mathbf{E} + \mathbf{E} \cdot \boldsymbol{\sigma}^0 \cdot \mathbf{E}^0 \rangle \\ & \quad - 2 \mathbf{E}^0 \cdot \boldsymbol{\sigma}^0 \cdot \mathbf{E}^0 \end{aligned} \quad (4)$$

or

$$\begin{aligned} \mathbf{E}^\infty \cdot (\bar{\boldsymbol{\sigma}} - \bar{\boldsymbol{\sigma}}^0) \cdot \mathbf{E}^\infty &= \langle \mathbf{E}^0 \cdot \Delta \boldsymbol{\sigma} \cdot \mathbf{E}^0 \rangle - \langle \Delta \mathbf{E} \cdot \boldsymbol{\sigma} \cdot \Delta \mathbf{E} \rangle \\ &+ \langle 2\mathbf{E} \cdot \boldsymbol{\sigma} \cdot \mathbf{E} - \mathbf{E}^0 \cdot \boldsymbol{\sigma} \cdot \mathbf{E} - \mathbf{E} \cdot \boldsymbol{\sigma} \cdot \mathbf{E}^0 \rangle \end{aligned} \quad (5)$$

where  $\Delta \boldsymbol{\sigma} = \boldsymbol{\sigma}(\mathbf{x}) - \boldsymbol{\sigma}^0(\mathbf{x})$  and  $\Delta \mathbf{E} = \mathbf{E}(\mathbf{x}) - \mathbf{E}^0(\mathbf{x})$ . It is easy to prove that the third terms on the right-hand sides of Eqs. (4) and (5) are identically zero under the given boundary condition. Therefore we have

$$\begin{aligned} \mathbf{E}^\infty \cdot (\bar{\boldsymbol{\sigma}} - \bar{\boldsymbol{\sigma}}^0) \cdot \mathbf{E}^\infty &= \langle \mathbf{E} \cdot \Delta \boldsymbol{\sigma} \cdot \mathbf{E} \rangle + \langle \Delta \mathbf{E} \cdot \boldsymbol{\sigma}^0 \cdot \Delta \mathbf{E} \rangle \\ &= \langle \mathbf{E}^0 \cdot \Delta \boldsymbol{\sigma} \cdot \mathbf{E}^0 \rangle - \langle \Delta \mathbf{E} \cdot \boldsymbol{\sigma} \cdot \Delta \mathbf{E} \rangle. \end{aligned} \quad (6)$$

Obviously, if  $\Delta \boldsymbol{\sigma}$  is positively definite, then  $\bar{\boldsymbol{\sigma}} - \bar{\boldsymbol{\sigma}}^0$  is also positively definite. From Eq. (6), we can obtain the following inequality:

$$\mathbf{E}^\infty \cdot (\bar{\boldsymbol{\sigma}} - \bar{\boldsymbol{\sigma}}^0) \cdot \mathbf{E}^\infty \leq \langle \mathbf{E}^0 \cdot \Delta \boldsymbol{\sigma} \cdot \mathbf{E}^0 \rangle. \quad (7)$$

In particular, if  $\boldsymbol{\sigma}(\mathbf{x})$ ,  $\boldsymbol{\sigma}^0(\mathbf{x})$ ,  $\bar{\boldsymbol{\sigma}}$ , and  $\bar{\boldsymbol{\sigma}}^0$  are all isotropic tensors, i.e.,

$$\boldsymbol{\sigma}(\mathbf{x}) = \sigma(\mathbf{x})\mathbf{I}, \quad \boldsymbol{\sigma}^0(\mathbf{x}) = \sigma^0(\mathbf{x})\mathbf{I}, \quad \bar{\boldsymbol{\sigma}} = \bar{\sigma}\mathbf{I}, \quad \bar{\boldsymbol{\sigma}}^0 = \bar{\sigma}^0\mathbf{I} \quad (8)$$

then Eq. (7) becomes

$$(\bar{\sigma} - \bar{\sigma}^0)(\mathbf{E}^\infty \cdot \mathbf{E}^\infty) \leq \langle \Delta \sigma(\mathbf{E}^0 \cdot \mathbf{E}^0) \rangle. \quad (9)$$

From Eq. (7) or Eq. (9), it is seen that the upper bound on the effective conductivity of the real material can be obtained through finding  $\mathbf{E}^0$  and  $\bar{\boldsymbol{\sigma}}^0$  for the comparison material.

Apply the boundary condition  $\mathbf{J}|_S = \mathbf{J}^\infty$  on the exterior boundaries of the RVEs of the real and comparison materials in Figs. 1(a) and 1(b), where  $\mathbf{J}^\infty$  is a constant flux vector. Then, we have

$$\langle \mathbf{J}(\mathbf{x}) \rangle = \langle \mathbf{J}_0(\mathbf{x}) \rangle = \mathbf{J}^\infty, \quad (10)$$

where  $\mathbf{J}(\mathbf{x})$  and  $\mathbf{J}_0(\mathbf{x})$  are the fluxes in the real and comparison materials, respectively. Following a procedure similar to that for obtaining Eq. (6), the following identity can be obtained:

$$\begin{aligned} \mathbf{J}^\infty \cdot (\bar{\boldsymbol{\rho}} - \bar{\boldsymbol{\rho}}_0) \cdot \mathbf{J}^\infty &= \langle \mathbf{J} \cdot \Delta \boldsymbol{\rho} \cdot \mathbf{J} \rangle + \langle \Delta \mathbf{J} \cdot \boldsymbol{\rho}_0 \cdot \Delta \mathbf{J} \rangle \\ &= \langle \mathbf{J}_0 \cdot \Delta \boldsymbol{\rho} \cdot \mathbf{J}_0 \rangle - \langle \Delta \mathbf{J} \cdot \boldsymbol{\rho} \cdot \Delta \mathbf{J} \rangle, \end{aligned} \quad (11)$$

where  $\Delta \boldsymbol{\rho} = \boldsymbol{\rho}(\mathbf{x}) - \boldsymbol{\rho}_0(\mathbf{x})$  and  $\Delta \mathbf{J} = \mathbf{J}(\mathbf{x}) - \mathbf{J}_0(\mathbf{x})$ .  $\bar{\boldsymbol{\rho}}$  and  $\bar{\boldsymbol{\rho}}_0$  are the effective resistivity tensors of the real and the comparison materials, respectively. From Eq. (11), it can be seen that if  $\Delta \boldsymbol{\rho}$  is positively definite, then  $\bar{\boldsymbol{\rho}} - \bar{\boldsymbol{\rho}}_0$  is also positively definite. It follows from the second equality in Eq. (11) that

$$\mathbf{J}^\infty \cdot (\bar{\boldsymbol{\rho}} - \bar{\boldsymbol{\rho}}_0) \cdot \mathbf{J}^\infty \leq \langle \mathbf{J}_0 \cdot \Delta \boldsymbol{\rho} \cdot \mathbf{J}_0 \rangle. \quad (12)$$

In particular, for an isotropic material, Eq. (12) reduces to

$$(\bar{\rho} - \bar{\rho}_0)(\mathbf{J}^\infty \cdot \mathbf{J}^\infty) \leq \langle \Delta \rho(\mathbf{J}_0 \cdot \mathbf{J}_0) \rangle. \quad (13)$$

It should be pointed out that although the above description is referred to as a heterogeneous medium consisting of a continuous matrix and discretely suspended spherical particles, the theoretical framework and the obtained inequalities in Eqs. (7) and (12) [(9) and (13) for the isotropic case] are actually applicable to composites with arbitrary micro-

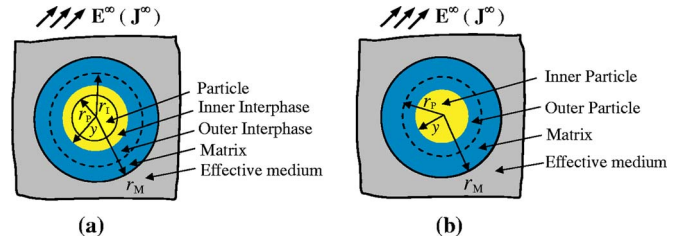


FIG. 2. (Color online) GSCM configurations for calculating the average quantities  $\langle \Delta \sigma(\mathbf{E}^0 \cdot \mathbf{E}^0) \rangle$  and  $\langle \Delta \rho(\mathbf{J}_0 \cdot \mathbf{J}_0) \rangle$ , and  $\bar{\boldsymbol{\sigma}}^0$  of the comparison materials of the two kinds of heterogeneous medium with a graded interphase (a) and with graded particles (b). For the meaning of  $y$  in (a) and (b) see the text.

structures and volume fractions of the constituents so long as the composites possess ergodicity, i.e., statistical homogeneity.<sup>15</sup> It is also seen that there are no restrictions on the microstructure of the comparison materials except the ergodicity. Thus the microstructure of a comparison material can be different from that of the real material. In practice, it is always expedient to choose a comparison material that facilitates the calculation of the quantities  $\bar{\boldsymbol{\sigma}}^0$ ,  $\bar{\boldsymbol{\rho}}_0$ ,  $\mathbf{E}^0$ , and  $\mathbf{J}_0$ . In the following part of this paper, we shall apply the above theoretical framework to macroscopically isotropic media containing discretely suspended spherical particles with a graded interphase or graded spherical particles, and give the corresponding bounds on the effective conductivities.

## B. Comparison materials and GSCM configuration

The radii of the spherical particles in both the material containing spherical particles with a graded interphase and that containing graded spherical particles without an interphase are denoted by  $r_p$ . For brevity, here and everywhere in this paper, all length scales are regarded as being normalized by the radius  $r_p$  of the spherical particles. Thus  $\mathbf{x}$  denotes the normalized position vector of a material point, and  $r$  denotes the normalized distance of a material point from the center of a spherical particle. All the constituents of the considered heterogeneous media are assumed to be isotropic. In the first kind of heterogeneous media, the conductivity of the graded interphase is assumed to vary in the radial direction. The outer radius of the graded interphase is denoted by  $r_i$ , as shown in Fig. 2(a). The comparison material is chosen to be an *ergodic* heterogeneous medium consisting of a continuous homogeneous matrix and discretely suspended spherical homogeneous particles [Fig. 1(b)]. The conductivities of the constituents of the comparison material are chosen in the following way. The conductivities of the particle and matrix regions are chosen to be the same as those of the particles and the matrix of the real material. The interphase region of the comparison material is divided into two concentric subregions, namely, the inner part and the outer part. The conductivity of the inner part is chosen to be  $\sigma^0 = \sigma_p$  ( $r_p \leq r \leq y, r_p \equiv 1$ ), where  $\sigma_p$  denotes the conductivity of the particles, and that of the outer part to be  $\sigma^0 = \sigma_M$  ( $y \leq r \leq r_i$ ) [Fig. 2(a)], where  $\sigma_M$  denotes the conductivity of the matrix. Hence the so-obtained comparison material is a two-phase heterogeneous medium consisting of the homogeneous ma-

trix and homogeneous particles, as shown in Fig. 1(b). The local intensity  $\mathbf{E}^0(\mathbf{x})$  and flux  $\mathbf{J}_0(\mathbf{x})$  in this two-phase heterogeneous medium, which are needed in the calculations of the bounds in Eqs. (9) and (13), are further calculated using the GSCM configuration in Fig. 2(a), which will be elaborated below.

In the second kind of heterogeneous medium, the conductivity of the particles is assumed to vary in the radial direction. The comparison material is obtained in the following way. A graded particle of radius  $r_p$  is divided into two concentric parts, namely, the inner part with a radius  $y$  and the outer part with the radius  $r_p$  [Fig. 2(b)]. The conductivity of the inner part can be chosen to be an arbitrary constant. In the calculations in this paper, it is chosen to be a constant which is either equal to the conductivity at the center of the original graded particle or equal to that at the dividing line  $r=y$ . The conductivity of the outer part, which is actually a spherical shell surrounding the inner particle, is chosen to be that of the matrix of the real material. Therefore it is seen that both of the comparison materials for the above two kinds of heterogeneous medium are a two-phase heterogeneous medium consisting of a homogeneous matrix and homogeneous spherical particles, as shown in Fig. 1(b).

As mentioned in Sec. II A, although the microstructure of a comparison material can be different from that of the considered real material, it is always expedient to choose a microstructure to facilitate the calculation. For the heterogeneous medium containing homogeneous spherical particles with a graded interphase, the conductivities of the particle and the matrix regions of the comparison material are chosen in such a way that  $\Delta\sigma=0$  in these regions; for the heterogeneous medium containing graded spherical particles, the conductivities of the particle and the matrix regions of the comparison material are chosen in such a way that  $\Delta\sigma=0$  in the matrix region. In this way, the calculations will be greatly simplified. Moreover, it is noted that a graded spherical particle can be regarded as an infinitesimal spherical particle with a graded interphase (the graded interphase starts from the center of the particle). However, as homogeneous particles with graded interphases may exist in many composites,<sup>23,28</sup> the cases for the graded interphase and graded particles are considered separately in this paper.

In order to get the bounds from the inequalities in Eqs. (9) and (13), we need to calculate the fields  $\mathbf{E}^0(\mathbf{x})$ ,  $\mathbf{J}_0(\mathbf{x})$ , and  $\bar{\sigma}^0(\bar{\rho}_0)$  in the above-mentioned two-phase comparison material. Many predictive schemes can be used to evaluate these quantities, and different schemes will produce different approximate values of  $\langle\Delta\sigma(\mathbf{E}^0 \cdot \mathbf{E}^0)\rangle$ ,  $\langle\Delta\rho(\mathbf{J}_0 \cdot \mathbf{J}_0)\rangle$  and  $\bar{\sigma}^0(\bar{\rho}_0)$ . In this paper, we will use the generalized self-consistent scheme<sup>39–42</sup> to evaluate  $\langle\Delta\sigma(\mathbf{E}^0 \cdot \mathbf{E}^0)\rangle$ ,  $\langle\Delta\rho(\mathbf{J}_0 \cdot \mathbf{J}_0)\rangle$  and  $\bar{\sigma}^0(\bar{\rho}_0)$  of the comparison material. The reason for this is as follows. The generalized self-consistent scheme, which was originally proposed by Kerner,<sup>39</sup> has been widely used in the literature to predict the effective elastic constants and conductivities of heterogeneous media containing spherical and ellipsoidal particles, and the GSCM predictions have been found to agree very well with the experimental data.<sup>40–43</sup> Weber *et al.*<sup>43</sup> studied the influence of the shape of randomly oriented, nonconducting inclusions in a conducting matrix on

the effective electrical conductivity, and found that the electric conductivity predicted by the GSCM agrees with the experimental results quite well. Moreover, Wu *et al.*<sup>38</sup> predicted the bounds on the effective elastic moduli of a composite containing spherical particles with a graded interphase using the average strain and stress, which are the counterparts of  $\langle\Delta\sigma(\mathbf{E}^0 \cdot \mathbf{E}^0)\rangle$  and  $\langle\Delta\rho(\mathbf{J}_0 \cdot \mathbf{J}_0)\rangle$  in the present conduction problem, calculated from the GSCM model of the comparison material. It is found that the obtained bounds very well bracket the effective moduli predicted by other schemes such as numerical computations and a differential scheme. Another reason for choosing the GSCM is that the predicted effective conductivity and the effective resistivity for a heterogeneous medium are reciprocal.

Following the above arguments, the GSCM configuration for the comparison material of the first kind of heterogeneous medium containing homogeneous particles with a graded interphase is shown in Fig. 2(a), and that for the comparison material of the second kind of heterogeneous medium containing graded particles is shown in Fig. 2(b). It is seen that both of these GSCM configurations consist of a homogeneous spherical particle of radius  $y$  embedded in a matrix shell of outer radius  $r_M$ , which is in turn embedded in an infinite effective medium, where  $r_M=y/f_p^{1/3}$ , and  $f_p$  is the volume fraction of the homogeneous particles in the comparison material. Hence, in the following, we shall calculate the average quantities  $\langle\Delta\sigma(\mathbf{E}^0 \cdot \mathbf{E}^0)\rangle$  and  $\langle\Delta\rho(\mathbf{J}_0 \cdot \mathbf{J}_0)\rangle$ , and  $\bar{\sigma}^0(\bar{\rho}_0)$  using these GSCM configurations.

Under a remote intensity field  $\mathbf{E}^\infty=E_z^\infty\mathbf{e}_z$  along the  $z$  axis, the local potential fields in the particle, the matrix and the effective medium in Figs. 2(a) and 2(b) are given by, in the spherical coordinate system,

$$\Phi_k = \left( F_k r + \frac{G_k}{r^2} \right) \cos \theta \quad (k = P, M, e), \quad (14)$$

where the sub- and superscripts  $P$ ,  $M$ , and  $e$  denote the particle, the matrix, and the effective medium in the GSCM configuration, respectively.  $G_P=0$  in the particle, and the constants  $F_P$ ,  $F_M$ ,  $G_M$ ,  $F_e$ , and  $G_e$  in Eq. (14) are determined by the following boundary and interface conditions in the GSCM configuration:

$$\begin{aligned} \Phi_P &= \Phi_M, & J_r^P &= J_r^M & \text{at } r=y, \\ \Phi_M &= \Phi_e, & J_r^M &= J_r^e & \text{at } r=r_M, \\ \Phi_e &= -E_z^\infty r \cos \theta & \text{at } r \rightarrow \infty, \end{aligned} \quad (15)$$

where  $J_r$  denotes the radial component of the flux. Based on the local potential in Eq. (14) and the interface and boundary conditions in Eq. (15), the local fields in the particle (with radius  $r=y$ ) and in the matrix (with outer radius  $r=r_M$ ) can be determined, and thus the effective conductivity  $\bar{\sigma}^0$  of the comparison material can be obtained

$$\bar{\sigma}^0 = \frac{\sigma_M[(1+2f_p)\sigma_P + 2(1-f_p)\sigma_M]}{(1-f_p)\sigma_P + (2+f_p)\sigma_M}, \quad (16)$$

where  $\sigma_P$  and  $\sigma_M$  are the conductivities of the homogeneous particle and matrix of the comparison material, respectively.

Hashin<sup>40</sup> has previously given the effective conductivity in Eq. (16) using the GSCM. For the GSCM configuration, the local intensity fields  $\mathbf{E}_P^0$  and  $\mathbf{E}_M^0$  in the particle and in the matrix under  $\mathbf{E}^\infty = E_z^\infty \mathbf{e}_z$  are, respectively,

$$\mathbf{E}_P^0 = A_{Pz} E_z^\infty \mathbf{e}_z, \quad \mathbf{E}_M^0 = E_z^\infty (A_{Mx} \mathbf{e}_x + A_{My} \mathbf{e}_y + A_{Mz} \mathbf{e}_z) \quad (17)$$

in which

$$\begin{aligned} A_{Pz} &= \frac{3\sigma_M}{H^0}, \quad A_{Mx} = \frac{3y^3 \sin 2\theta(\sigma_P - \sigma_M)}{2r^3 H^0} \cos \varphi, \\ A_{My} &= \frac{3y^3 \sin 2\theta(\sigma_P - \sigma_M)}{2r^3 H^0} \sin \varphi, \\ A_{Mz} &= \frac{1}{H^0} \left[ \sigma_P + 2\sigma_M + \frac{(1 + 3 \cos 2\theta)y^3}{2r^3} (\sigma_P - \sigma_M) \right], \end{aligned} \quad (18)$$

where  $H^0 = (1 - f_P)\sigma_P + (2 + f_P)\sigma_M$ .  $\mathbf{e}_x$ ,  $\mathbf{e}_y$ , and  $\mathbf{e}_z$  are the unit base vectors of the Cartesian coordinate system, and  $r$  ( $y \leq r \leq r_M$ ) is the radial distance from the origin. The local flux fields  $\mathbf{J}_0^P$  and  $\mathbf{J}_0^M$  in the particle and in the matrix under a remote field  $\mathbf{J}^\infty = J_z^\infty \mathbf{e}_z$  are, respectively,

$$\mathbf{J}_0^P = C_{Pz} J_z^\infty \mathbf{e}_z, \quad \mathbf{J}_0^M = J_z^\infty (C_{Mx} \mathbf{e}_x + C_{My} \mathbf{e}_y + C_{Mz} \mathbf{e}_z) \quad (19)$$

in which

$$\begin{aligned} C_{Pz} &= \frac{3\sigma_P}{H_0}, \quad C_{Mx} = \frac{3y^3 \sin 2\theta(\sigma_P - \sigma_M)}{2r^3 H_0} \cos \varphi, \\ C_{My} &= \frac{3y^3 \sin 2\theta(\sigma_P - \sigma_M)}{2r^3 H_0} \sin \varphi, \\ C_{Mz} &= \frac{1}{H_0} \left[ \sigma_P + 2\sigma_M + \frac{(1 + 3 \cos 2\theta)y^3}{2r^3} (\sigma_P - \sigma_M) \right], \end{aligned} \quad (20)$$

where  $H_0 = (1 + 2f_P)\sigma_P + 2(1 - f_P)\sigma_M$ .

From the above results, it is seen that the formulas in Eqs. (9) and (16)–(18) constitute the equations to obtain the upper bound on the effective conductivity of the real material; and those in Eqs. (13), (16), (19), and (20) constitute the equations to obtain the lower bound with  $\bar{\rho}_0 = 1/\bar{\sigma}^0$ . However, the bounds so obtained rely on the value of  $y$ . For this reason, the bounds can be optimized by altering  $y$ . This will be illustrated in the following.

### III. APPLICATION TO SPHERICAL PARTICLES WITH GRADED INTERPHASE

#### A. Optimized bounds for graded interphase

As indicated above, the interphase region of the comparison material is divided into two concentric subregions, namely, the inner part ( $\sigma^0 = \sigma_P$ ,  $r_P \leq r \leq y$ ) and the outer part ( $\sigma^0 = \sigma_M$ ,  $y \leq r \leq r_I$ ). In this case,  $\Delta\sigma = 0$  in the particle and the matrix, and  $\Delta\sigma \neq 0$  in the interphase zone. Therefore Eq. (9) can be expressed as

$$\bar{\sigma} \leq \bar{\sigma}^0 + B_I(y), \quad (21)$$

$$\begin{aligned} B_I(y) &= \frac{f_I}{(\mathbf{E}^\infty \cdot \mathbf{E}^\infty)} \langle \Delta\sigma(\mathbf{E}^0 \cdot \mathbf{E}^0) \rangle_I \\ &= \frac{1}{(\mathbf{E}^\infty \cdot \mathbf{E}^\infty)} \{ f_{IP} \langle \Delta\sigma(\mathbf{E}_P^0 \cdot \mathbf{E}_P^0) \rangle_{IP} \\ &\quad + f_{IM} \langle \Delta\sigma(\mathbf{E}_M^0 \cdot \mathbf{E}_M^0) \rangle_{IM} \}. \end{aligned} \quad (22)$$

Here,  $f_I = (r_I^3 - r_P^3)/r_M^3$  is the volume fraction of the graded interphases in the real material,  $f_{IP} = (y^3 - r_P^3)/r_M^3$ , and  $f_{IM} = (r_I^3 - y^3)/r_M^3$ .  $\langle \cdot \rangle_I$  denotes the volume average over the entire interphase ( $r_P \leq r \leq r_I$ ),  $\langle \cdot \rangle_{IP}$  denotes the volume average over the inner interphase ( $r_P \leq r \leq y$ ), and  $\langle \cdot \rangle_{IM}$  the volume average over the outer interphase ( $y \leq r \leq r_I$ ). Thus  $\bar{\sigma}^0$ ,  $B_I$ ,  $\mathbf{E}_P^0$ , and  $\mathbf{E}_M^0$  are all functions of  $y$ . Under  $\mathbf{E}^\infty = E_z^\infty \mathbf{e}_z$ ,  $B_I(y)$  in Eq. (22) can be simplified using Eqs. (17) and (18)

$$B_I(y) = f_{IP} \langle \Delta\sigma A_{Pz}^2 \rangle_{IP} + f_{IM} \langle \Delta\sigma (A_{Mx}^2 + A_{My}^2 + A_{Mz}^2) \rangle_{IM}. \quad (23)$$

Let the parameter  $y$  vary between  $r_P$  and  $r_I$ , namely, let  $f_P$  vary between  $f_R$  and  $f_R + f_I$ , where  $f_R$  is the volume fraction of the homogeneous particles in the real material, to give the minimum value of the quantity on the right side of Eq. (21). Then the optimized upper bound  $\bar{\sigma}^{\text{upp}}$  on  $\bar{\sigma}$  can be obtained

$$\bar{\sigma}^{\text{upp}} = \min_{(r_P \leq y \leq r_I)} \{ \bar{\sigma}^0(y) + B_I(y) \}. \quad (24)$$

Likewise, the lower bound on the effective conductivity of the composite with the graded interphase can be obtained from Eq. (13),

$$\bar{\sigma} \geq \frac{1}{\bar{\rho}_0 + B'_I(y)}, \quad (25)$$

in which

$$\begin{aligned} B'_I(y) &= \frac{f_I}{(\mathbf{J}^\infty \cdot \mathbf{J}^\infty)} \langle \Delta\rho(\mathbf{J}_0 \cdot \mathbf{J}_0) \rangle_I \\ &= \frac{1}{(\mathbf{J}^\infty \cdot \mathbf{J}^\infty)} \{ f_{IP} \langle \Delta\rho(\mathbf{J}_0^P \cdot \mathbf{J}_0^P) \rangle_{IP} + f_{IM} \langle \Delta\rho(\mathbf{J}_0^M \cdot \mathbf{J}_0^M) \rangle_{IM} \}. \end{aligned} \quad (26)$$

In Eqs. (25) and (26),  $\bar{\rho}_0$  ( $\bar{\rho}_0 = 1/\bar{\sigma}^0$ ),  $\bar{\sigma}^0$ , and  $B'_I$  are all functions of  $y$ . Under  $\mathbf{E}^\infty = E_z^\infty \mathbf{e}_z$ ,  $B'_I(y)$  in Eq. (26) can be simplified using Eqs. (19) and (20)

$$B'_I(y) = f_{IP} \langle \Delta\sigma C_{Pz}^2 \rangle_{IP} + f_{IM} \langle \Delta\sigma (C_{Mx}^2 + C_{My}^2 + C_{Mz}^2) \rangle_{IM}. \quad (27)$$

Let the parameter  $y$  vary between  $r_P$  and  $r_I$  to give the maximum value of the quantity on the right side of Eq. (25). Then the optimized lower bound  $\bar{\sigma}_{\text{low}}$  on  $\bar{\sigma}$  can be obtained

$$\bar{\sigma}_{\text{low}} = \max_{(r_P \leq y \leq r_I)} \left\{ \frac{\bar{\sigma}^0(y)}{1 + \bar{\sigma}^0(y) B'_I(y)} \right\}. \quad (28)$$

Therefore, given a conductivity profile of the graded interphase, the optimized upper and lower bounds can be obtained from Eqs. (16), (23), (24), (27), and (28). The procedure is simple and easy to follow. In the following, some

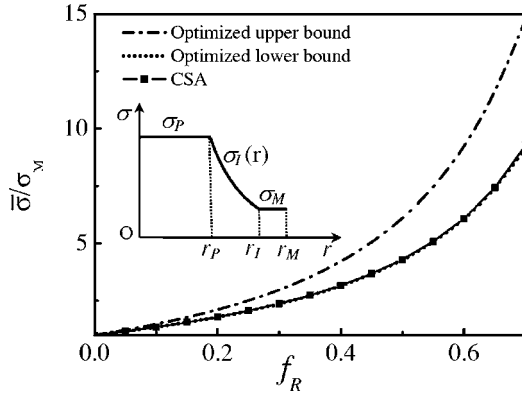


FIG. 3. Bounds and CSA prediction of the normalized effective conductivity  $\bar{\sigma}/\sigma_M$  of a heterogeneous medium containing spherical particles with a graded interphase [ $\sigma_I(r)=\sigma_p r^Q$ ,  $\sigma_p=20\sigma_M$ ,  $t=0.1$ ].  $f_R$  denotes the volume fraction of the particles in the heterogeneous medium.

numerical results of the optimized bounds will be shown and also compared with those obtained using the composite sphere assemblage (CSA) model. The details of the CSA model are given in the Appendix.

#### B. Examples of graded interphases

We consider two heterogeneous media with different contrasts between the conductivities of the matrix and particles. In one medium, the conductivity of the particles is higher than that of the matrix ( $\sigma_p=20\sigma_M$ ), and the ratio of the thickness of the interphase to the radius of the particles is  $t=0.1$ . In another, the conductivity of the particles is lower than that of the matrix ( $\sigma_p=\sigma_M/20$ ), and  $t$  is also 0.1. In both of these heterogeneous media, the conductivity profile of the interphase is depicted by a simple power-law  $\sigma_I(r)=\sigma_p r^Q$  ( $r_p \leq r \leq r_l$ ), where  $Q$  is a power exponent. However, the constant  $Q$  is determined by the condition  $\sigma_I|_{r=r_l}=\sigma_M$ .

The numerical results of the bounds for these two heterogeneous media are shown in Figs. 3 and 4, respectively. It can be seen from Fig. 3 that the optimized lower bound and

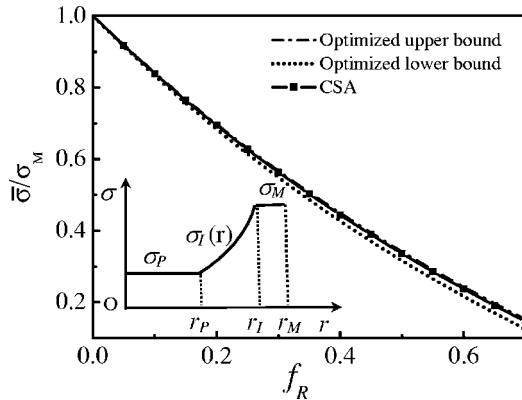


FIG. 4. Bounds and CSA prediction of the normalized effective conductivity  $\bar{\sigma}/\sigma_M$  of a heterogeneous medium containing spherical particles with a graded interphase [ $\sigma_I(r)=\sigma_p r^Q$ ,  $\sigma_p=\sigma_M/20$ ,  $t=0.1$ ].

the CSA are numerically indistinguishable from each other for the case of  $\sigma_p=20\sigma_M$ . For the case of  $\sigma_p=\sigma_M/20$ , the optimized upper bound and the CSA are numerically indistinguishable from each other (Fig. 4).

### IV. APPLICATION TO GRADED SPHERICAL PARTICLES

#### A. Optimized bounds for graded particles

The effective conductivity of the heterogeneous medium containing graded particles can be bounded by Eq. (9)

$$\bar{\sigma} \leq \bar{\sigma}^0 + B_p(y), \quad (29)$$

in which

$$\begin{aligned} B_p(y) &= \frac{f_R}{(\mathbf{E}^\infty \cdot \mathbf{E}^\infty)} \langle \Delta \sigma (\mathbf{E}^0 \cdot \mathbf{E}^0) \rangle_P \\ &= \frac{1}{(\mathbf{E}^\infty \cdot \mathbf{E}^\infty)} \{ f_{PP} \langle \Delta \sigma (\mathbf{E}_P^0 \cdot \mathbf{E}_P^0) \rangle_{PP} \\ &\quad + f_{PM} \langle \Delta \sigma (\mathbf{E}_M^0 \cdot \mathbf{E}_M^0) \rangle_{PM} \} \\ &= f_{PP} \langle \Delta \sigma A_{Pz}^2 \rangle_{PP} + f_{PM} \langle \Delta \sigma (A_{Mx}^2 + A_{My}^2 + A_{Mz}^2) \rangle_{PM}. \end{aligned} \quad (30)$$

Here,  $f_R=r_p^3/r_M^3$  is the volume fraction of the graded particles in the real material,  $f_{PP}=y^3/r_M^3$  and  $f_{PM}=(r_p^3-y^3)/r_M^3$ .  $\langle \cdot \rangle_P$  denotes the volume average over the particle ( $0 \leq r \leq r_p$ ),  $\langle \cdot \rangle_{PP}$  denotes the volume average over the inner part of the particle ( $0 \leq r \leq y$ ), and  $\langle \cdot \rangle_{PM}$  denotes the volume average over the outer part of the particle ( $y \leq r \leq r_p$ ). In this case,  $\bar{\sigma}^0$  and  $B_p(y)$  are all functions of  $y$ . Letting  $y$  vary between 0 and  $r_p$  (i.e.,  $0 \leq f_p \leq f_R$ ) to give the minimum value of the quantity on the right side of Eq. (29), then the optimized upper bound  $\bar{\sigma}^{\text{upp}}$  on  $\bar{\sigma}$  can be obtained

$$\bar{\sigma}^{\text{upp}} = \min_{(0 \leq y \leq r_p)} \{ \bar{\sigma}^0(y) + B_p(y) \}. \quad (31)$$

The lower bound can be obtained from the inequality

$$\bar{\sigma} \geq \frac{1}{\bar{\rho}_0 + B'_p(y)} \quad (32)$$

in which

$$\begin{aligned} B'_p(y) &= \frac{f_R}{(\mathbf{J}^\infty \cdot \mathbf{J}^\infty)} \langle \Delta \rho (\mathbf{J}_0 \cdot \mathbf{J}_0) \rangle_P \\ &= \frac{1}{(\mathbf{J}^\infty \cdot \mathbf{J}^\infty)} \{ f_{PP} \langle \Delta \rho (\mathbf{J}_0^P \cdot \mathbf{J}_0^P) \rangle_{PP} + f_{PM} \langle \Delta \rho (\mathbf{J}_0^M \cdot \mathbf{J}_0^M) \rangle_{PM} \} \\ &= f_{PP} \langle \Delta \sigma C_{Pz}^2 \rangle_{PP} + f_{PM} \langle \Delta \sigma (C_{Mx}^2 + C_{My}^2 + C_{Mz}^2) \rangle_{PM}. \end{aligned} \quad (33)$$

In Eqs. (32) and (33),  $\bar{\rho}_0$  ( $\bar{\rho}_0=1/\bar{\sigma}^0$ ),  $\bar{\sigma}^0$ , and  $B'_p(y)$  are all functions of  $y$ . Letting  $y$  vary between 0 and  $r_p$  to give the maximum value of the quantity on the right side of Eq. (32), then the optimized lower bound  $\bar{\sigma}_{\text{low}}$  on  $\bar{\sigma}$  can be obtained

$$\bar{\sigma}_{\text{low}} = \max_{(0 \leq y \leq r_p)} \left\{ \frac{\bar{\sigma}^0(y)}{1 + \bar{\sigma}^0(y) B'_p(y)} \right\}. \quad (34)$$

TABLE I. Comparison of the optimized upper and lower bounds, the CSA, and the prediction of Wei *et al.* (Ref. 18) for graded spherical particles with a linear dielectric profile  $\sigma_P(r)=\sigma_M(b+cr)$  at  $f_R=0.1$  and  $f_R=0.5$ .

$b/c$	$f_R=0.1$			$f_R=0.5$			
	Upper	Lower	Wei <i>et al.</i> (Ref. 18)	CSA	Upper	Lower	CSA
1	1.06213	1.05844	1.06006	1.06074	1.33673	1.32066	1.33048
10	1.24844	1.24838	1.24787	1.24840	2.85742	2.85687	2.85706
20	1.28520	1.28519	1.28488	1.28520	3.30104	3.30092	3.30095
30	1.29975	1.29975	1.29952	1.29975	3.49653	3.49649	3.4965
40	1.30754	1.30754	1.30737	1.30754	3.60657	3.60655	3.60655
50	1.31240	1.31240	1.31226	1.31240	3.67714	3.67713	3.67713
60	1.31572	1.31572	1.31560	1.31572	3.72624	3.72623	3.72623
70	1.31813	1.31813	1.31803	1.31813	3.76238	3.76237	3.76238

Therefore, given a conductivity profile of the graded particles, the optimized upper and lower bounds can be obtained from Eqs. (16), (30), (31), (33), and (34). In the following, some numerical results of the optimized bounds will be shown and also compared with those obtained using the composite sphere assemblage (CSA) model.

**B. Examples of graded particles**

Using the Landau’s formula,<sup>5</sup> Wei *et al.*<sup>18</sup> predicted the effective dielectric constant of a heterogeneous medium containing graded spherical particles with a linear dielectric profile  $\sigma_P(r)=\sigma_M(b+cr)$  (where  $b$  and  $c$  are two constants). However, the prediction of Wei *et al.*<sup>18</sup> is only valid for low volume fractions of the particles. As mentioned in the beginning of Sec. II A, the present theory is also applicable to the prediction of the effective dielectric constants of heterogeneous media. Table I shows the numerical results calculated from the optimized upper and lower bounds, the CSA model, and those of Wei *et al.*<sup>18</sup> for the considered medium. For different ratios of  $b/c$ , the numerical results of the optimized upper and lower bounds, the CSA prediction, and those of

Wei *et al.*<sup>18</sup> are practically identical at  $f_R=0.1$ . At  $f_R=0.5$ , the numerical results of the optimized upper and lower bounds and those predicted by the CSA are also practically identical.

We further compare the optimized bounds with the CSA for a heterogeneous medium containing graded particles with a general power-law conductivity profile  $\sigma_P(r)=c\sigma_M(b+r)^Q$ . Figure 5 shows the variations of the bounds and the CSA prediction as functions of the power exponent  $Q$  at  $f_R=0.5$ . The optimized bounds and the CSA are very close to each other. Moreover, the data predicted by the CSA are always within the bounds, albeit very narrow. Figure 6 shows the variations of the optimized bounds and CSA prediction as functions of the volume fraction of the particles for  $c=100$ ,  $b=1$ , and  $Q=-3$ . It is seen that the CSA prediction is always within the bounds.

**V. CONCLUDING REMARKS**

In this paper, through introducing comparison materials with homogeneous constituents, the bounds on the effective conductivities of heterogeneous media containing homoge-

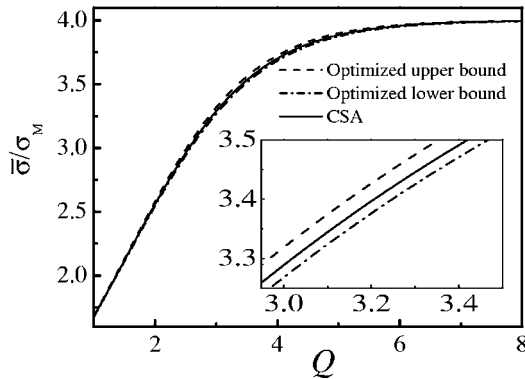


FIG. 5. Bounds and CSA prediction of the normalized effective conductivity  $\bar{\sigma}/\sigma_M$  of a heterogeneous medium containing graded spherical particles with the conductivity profile  $\sigma_P(r)=c\sigma_M(b+r)^Q$  as functions of the exponent  $Q$  ( $c=1$ ,  $b=2$ , and  $f_R=0.5$ ).

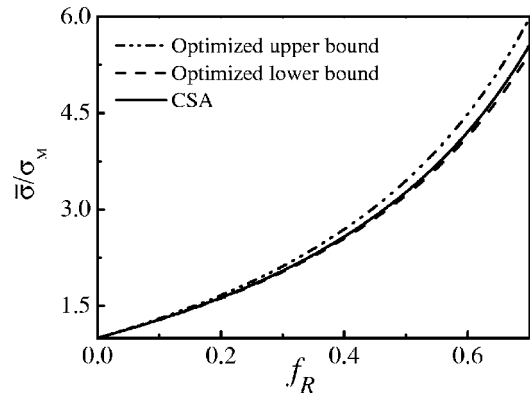


FIG. 6. Bounds and CSA prediction of the normalized effective conductivity  $\bar{\sigma}/\sigma_M$  of a heterogeneous medium containing graded spherical particles with the conductivity profile  $\sigma_P(r)=c\sigma_M(b+r)^Q$  as functions of the volume fraction  $f_R$  ( $c=100$ ,  $b=1$ , and  $Q=-3$ ).

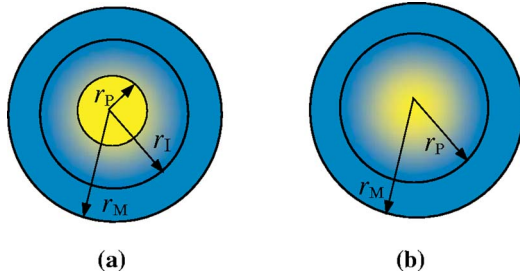


FIG. 7. (Color online) Configurations of the CSA model for heterogeneous media with graded interphase (a) and graded particles (b).

neous particles with a graded interphase or graded particles are presented. The comparison materials provide a means of obtaining optimized bounds. The effective conductivities of these heterogeneous media are also predicted using the composite sphere assemblage (CSA) model. It is shown that the CSA predictions are within the appropriate bounds for the considered materials. Although the studies in this paper are for graded heterogeneous media with linear properties, the results can be useful in the studies of the effective constitutive relations of nonlinear heterogeneous media following the theoretical framework based on the concept of *linear comparison materials*, as demonstrated, for example, in the work of Ponte Castañeda.<sup>12</sup> Moreover, the present theory can be extended to the following cases: anisotropic and graded spherical particles/interphases and graded ellipsoidal particles/interphases. It is emphasized that in this paper, we only consider *ergodic* heterogeneous media. Thus the theoretical framework based upon the comparison material presented in Sec. II A is applicable to composites with arbitrary microstructures and volume fractions of the constituents so long as the composites possess ergodicity, and the microstructure of a comparison material can be different from that of the real material. For statistically inhomogeneous materials, the effective conductivities need to be predicted by other methods based upon the microstructural information.<sup>16</sup>

#### ACKNOWLEDGMENT

This work was supported by the National Natural Science Foundation of China under Grant No. 10525209.

#### APPENDIX

The configuration of the composite sphere assemblage (CSA) model for the heterogeneous medium containing homogeneous particles with a graded interphase consists of three concentric spheres with radii  $r=r_p$ ,  $r=r_I$ , and  $r=r_M$  [Fig. 7(a)], which correspond to the radius of the particle, the outer radius of the graded interphase, and the outer radius of the matrix shell, respectively. The boundary conditions are imposed at the outer boundary of the matrix shell ( $r=r_M$ ). The configuration of the CSA for the heterogeneous medium containing graded particles consists of two concentric spheres with radii  $r=r_p$  and  $r=r_M$  [Fig. 7(b)], which correspond to the radius of the graded particle and the outer radius

of the matrix shell, respectively. The boundary conditions are imposed at the outer boundary of the matrix shell ( $r=r_M$ ).

Applying an intensity (or a flux) field along the  $z$  axis on the boundary of  $r=r_M$ , the boundary and the interface conditions of the CSA model for the graded interphase are [Fig. 7(a)], in the spherical coordinate system,

$$\Phi_P = \Phi_I, \quad J_r^P = J_r^I \quad \text{at } r = r_p,$$

$$\Phi_I = \Phi_M, \quad J_r^I = J_r^M \quad \text{at } r = r_I,$$

$$\Phi_M = -\beta r_M \cos \theta, \quad J_r^M = \bar{\sigma} \beta \cos \theta \quad \text{at } r = r_M, \quad (\text{A1})$$

where the sub- and superscripts  $P$ ,  $I$ , and  $M$  denote the particle, the interphase, and the matrix, respectively. For a graded interphase with a property profile depicted by a simple power-law  $\sigma_I(r) = \sigma_P r^Q$ , where  $Q$  is a power exponent, the local potential field in the graded interphase is

$$\Phi_I = (F_I r^{D_1} + G_I r^{D_2}) \cos \theta, \quad (\text{A2})$$

where

$$D_1 = \frac{1}{2}[-Q - 1 + \sqrt{(Q+1)^2 + 8}],$$

and

$$D_2 = \frac{1}{2}[-Q - 1 - \sqrt{(Q+1)^2 + 8}].$$

The local potential fields in the particle and the matrix are given by Eq. (14), and the constants  $F_P$ ,  $F_I$ ,  $G_I$ ,  $F_M$ , and  $G_M$  in Eqs. (A2) and (14) are determined by the boundary and interface conditions in Eq. (A1), whereas  $G_P = 0$ . With the solution of the fields, the effective conductivity of the composite sphere with the graded interphase can be obtained.

Applying an intensity (or a flux) field along the  $z$  axis on the boundary of  $r=r_M$ , the interface and boundary conditions of the CSA model for the graded particle are [Fig. 7(b)]

$$\Phi_P = \Phi_M, \quad J_r^P = J_r^M \quad \text{at } r = r_p,$$

$$\Phi_M = -\beta r_M \cos \theta, \quad J_r^M = \bar{\sigma} \beta \cos \theta \quad \text{at } r = r_M. \quad (\text{A3})$$

For a particle with a conductivity depicted by a power-law  $\sigma_P(r) = c \sigma_M (b+r)^Q$ , where  $b$  and  $c$  are two constants, the local potential in the graded particle is<sup>44</sup>

$$\Phi_P = F_P F \left( \alpha_1, \beta_1, \gamma_1, -\frac{r}{b} \right) r \cos \theta, \quad (\text{A4})$$

where

$$\alpha_1 = \frac{1}{2}[Q + 3 - \sqrt{(Q+1)^2 + 8}],$$

$$\beta_1 = \frac{1}{2}[Q + 3 + \sqrt{(Q+1)^2 + 8}],$$

$\gamma_1 = 4$ , and  $F(\alpha_1, \beta_1, \gamma_1, -\frac{r}{b})$  is the hypergeometric function.<sup>45</sup> In the matrix, the local potential is still given by Eq. (14). The constants  $F_P$ ,  $F_M$ , and  $G_M$  in Eqs. (14) and (A4) are determined by the boundary and interface conditions in Eq. (A3). Then the effective conductivity  $\bar{\sigma}$  of the composite sphere with the graded particle can be obtained.

\*Author to whom correspondence should be addressed. Electronic address: jxwang@pku.edu.cn

- <sup>1</sup>J. C. Maxwell, *Treatise on Electricity and Magnetism* (Clarendon Press, Oxford, 1873).
- <sup>2</sup>J. W. Rayleigh, *Philos. Mag.* **34**, 481 (1892).
- <sup>3</sup>A. Einstein, *Ann. Phys.* **19**, 289 (1905).
- <sup>4</sup>R. Landauer, *J. Appl. Phys.* **23**, 779 (1952).
- <sup>5</sup>L. D. Landau and E. M. Lifshitz, *Electrodynamics of Continuous Media* (Pergamon, Oxford, 1960).
- <sup>6</sup>Z. Hashin and S. Shtrikman, *J. Appl. Phys.* **33**, 3125 (1962).
- <sup>7</sup>S. Torquato, *J. Chem. Phys.* **84**, 6345 (1986).
- <sup>8</sup>D. J. Bergman, *Solid State Phys.* **46**, 147 (1992).
- <sup>9</sup>S. Torquato and M. D. Rintoul, *Phys. Rev. Lett.* **75**, 4067 (1995).
- <sup>10</sup>R. W. Zimmerman, *Proc. R. Soc. London, Ser. A* **452**, 1713 (1996).
- <sup>11</sup>C. W. Nan and R. Birringer, *Phys. Rev. B* **57**, 8264 (1998).
- <sup>12</sup>P. Ponte Castañeda, *Phys. Rev. B* **57**, 12077 (1998).
- <sup>13</sup>P. Ponte Castañeda, *Phys. Rev. B* **64**, 214205 (2001).
- <sup>14</sup>G. W. Milton, *The Theory of Composites* (Cambridge University Press, Cambridge, England, 2002).
- <sup>15</sup>S. Torquato, *Random Heterogeneous Materials: Microstructure and Macroscopic Properties* (Springer-Verlag, New York, 2002).
- <sup>16</sup>J. Quintanilla and S. Torquato, *Phys. Rev. E* **55**, 1558 (1997).
- <sup>17</sup>L. Dong, G. Q. Gu, and K. W. Yu, *Phys. Rev. B* **67**, 224205 (2003).
- <sup>18</sup>E. B. Wei, Z. D. Yang, and J. B. Song, *Phys. Lett. A* **316**, 419 (2003).
- <sup>19</sup>L. Dong, J. P. Huang, K. W. Yu, and G. Q. Gu, *J. Appl. Phys.* **95**, 621 (2004).
- <sup>20</sup>J. P. Huang and K. W. Yu, *Appl. Phys. Lett.* **85**, 94 (2004).
- <sup>21</sup>J. P. Huang, M. Karttunen, K. W. Yu, L. Dong, and G. Q. Gu, *Phys. Rev. E* **69**, 051402 (2004).
- <sup>22</sup>L. Gao, J. P. Huang, and K. W. Yu, *Phys. Rev. B* **69**, 075105 (2004).
- <sup>23</sup>M. P. Lutz and R. W. Zimmerman, *Int. J. Solids Struct.* **42**, 429 (2005).
- <sup>24</sup>S. Suresh, *Science* **292**, 2447 (2001).
- <sup>25</sup>A. Kawasaki and R. Watanabe, *Ceram. Int.* **23**, 73 (1997).
- <sup>26</sup>K. Jayaraman and K. L. Reifsnider, *J. Compos. Mater.* **26**, 770 (1992).
- <sup>27</sup>J. P. Huang, K. W. Yu, G. Q. Gu, and M. Karttunen, *Phys. Rev. E* **67**, 051405 (2003).
- <sup>28</sup>M. Ostoja-Starzewski, I. Jasiuk, W. Wang, and K. Alzebdeh, *Acta Mater.* **44**, 2057 (1996).
- <sup>29</sup>L. J. Lauhon, M. S. Gudixsen, C. L. Wang, and C. M. Lieber, *Nature (London)* **420**, 57 (2002).
- <sup>30</sup>R. E. Bailey and S. M. Nie, *J. Am. Chem. Soc.* **125**, 7100 (2003).
- <sup>31</sup>M. Abe and T. Suwa, *Phys. Rev. B* **70**, 235103 (2004).
- <sup>32</sup>Y. C. Li, M. F. Ye, C. H. Yang, X. H. Li, and Y. F. Li, *Adv. Funct. Mater.* **15**, 433 (2005).
- <sup>33</sup>A. V. Goncharenko, *Chem. Phys. Lett.* **386**, 25 (2004).
- <sup>34</sup>H.-C. Weissker, J. Furthmuller, and F. Bechstedt, *Phys. Rev. B* **67**, 165322 (2003).
- <sup>35</sup>A. J. Williamson and A. Zunger, *Phys. Rev. B* **59**, 15819 (1999).
- <sup>36</sup>K. Rajeshwar, N. R. Tacconi, and C. R. Chenthamarakshan, *Chem. Mater.* **13**, 2765 (2001).
- <sup>37</sup>S. Y. Lu, M. L. Wu, and H. L. Chen, *J. Appl. Phys.* **93**, 5789 (2003).
- <sup>38</sup>Y. M. Wu, Z. P. Huang, Y. Zhong, and J. Wang, *Compos. Sci. Technol.* **64**, 1345 (2004).
- <sup>39</sup>E. H. Kerner, *Proc. Phys. Soc. London, Sect. B* **69**, 802 (1956).
- <sup>40</sup>Z. Hashin, *J. Compos. Mater.* **3**, 284 (1968).
- <sup>41</sup>T. Miloh and Y. Benveniste, *J. Appl. Phys.* **63**, 789 (1988).
- <sup>42</sup>R. M. Christensen, *J. Mech. Phys. Solids* **38**, 379 (1990).
- <sup>43</sup>L. Weber, C. Fischer, and A. Mortensen, *Acta Mater.* **51**, 495 (2003).
- <sup>44</sup>E. B. Wei, Y. M. Poon, and F. G. Shin, *Phys. Lett. A* **336**, 264 (2005).
- <sup>45</sup>G. B. Arfken and H. J. Weber, *Mathematical Methods for Physicists*, 5th ed. (Harcourt/Academic Press, San Diego, 2001).